Progress In Electromagnetics Research C, Vol. 128, 113–127, 2023

Design and Analysis of Multi-Layer Coils to Enhance Performance of Spread Resonance Based MI Waveguide System

Sandeep N. Dandu[1], Vinay Kumar[2, *], and Joydeep Sengupta[1]

Abstract—In this work, we analytically enhanced the channel capacity and bandwidth of an MI waveguide system by using multi-layer coils (MLCs) and spread resonance strategy. In this analysis, we considered the practical constraints like parasitic capacitance, ac resistance, skin and proximity effects, and inductance of multi-layer coil. The bandwidth is significantly enhanced up to 6 kHz, and a trade-off is observed between the bandwidth and achievable transmission range. Besides, the influence of coil turns, layers, and the impact of spread intensity are analyzed. Furthermore, we introduced a new MLC structure with thin-rectangular cross section which has promising characteristics like higher magnetic flux, low ac resistance, and high inductance. The performance of this coil is compared with that of existing round circular and tubular multi-layer coils. These characteristics are comparatively studied through simulations performed in ANSYS Maxwell R21. Based on the results we infer that the proposed coil is more advantageous than the existing standard MLC for MI communication in terms of cost and system performance.

1. INTRODUCTION

Magnetic Induction communication (MI) is an emerging communication technique for non-conventional media like underground and underwater. In traditional communication technique, the radio frequency (RF) signals attenuate rapidly due to dynamic channel nature and experience high path loss, low data rate, and high propagation delay [1, 2]. Contrary to this, MI technique is promising in this media due to constant channel behavior and small antenna size requirement. It finds applications in gas pipeline monitoring, underground mine disaster detection, border sensing, and so on [3–5]. In MI technique, the coil itself acts as an antenna, and it basically works on the principle of transformer wherein the signal gets transferred from one coil to another by means of mutual induction between adjacent coils [6, 7].

Initially, the communication is established between two coils in which one coil acts as a transmitter and the other as a receiver. The communication range offered by such a setup is up to 10 m. To enhance the communication range, a waveguide technique is developed by means of which the communication range is extended up to a few hundreds of meters [8, 9]. This MI waveguide is different from the traditional RF waveguide which is a small continuous physical structure. The MI waveguide comprises a transmitter coil and a receiver coil separated by several relay coils, as shown in Fig. 1. As shown in this figure, the MI transmitter has three components. At first, the encoder converts the source data to digital form for further processing. Then the encoded signal modulates the carrier signal based on a suitable modulation technique. Finally, the signal is transmitted through an MI coil. After going through a series of relay coils, at the receiver, the MI signal is detected, and subsequently, the data is demodulated and decoded in the succeeding circuitry. Herein, the transmitter and receiver coils

Received 9 November 2022, Accepted 20 December 2022, Scheduled 3 January 2023
* Corresponding author: Vinay Kumar (vinay.k@mnnit.ac.in).
[1] The Department of Electronics and Communications Engineering, Visvesvaraya National Institute of Technology, Nagpur 440010, India. [2] Department of Electronics and Communications Engineering, Motilal Nehru National Institute of Technology, Prayagraj 211004, India.

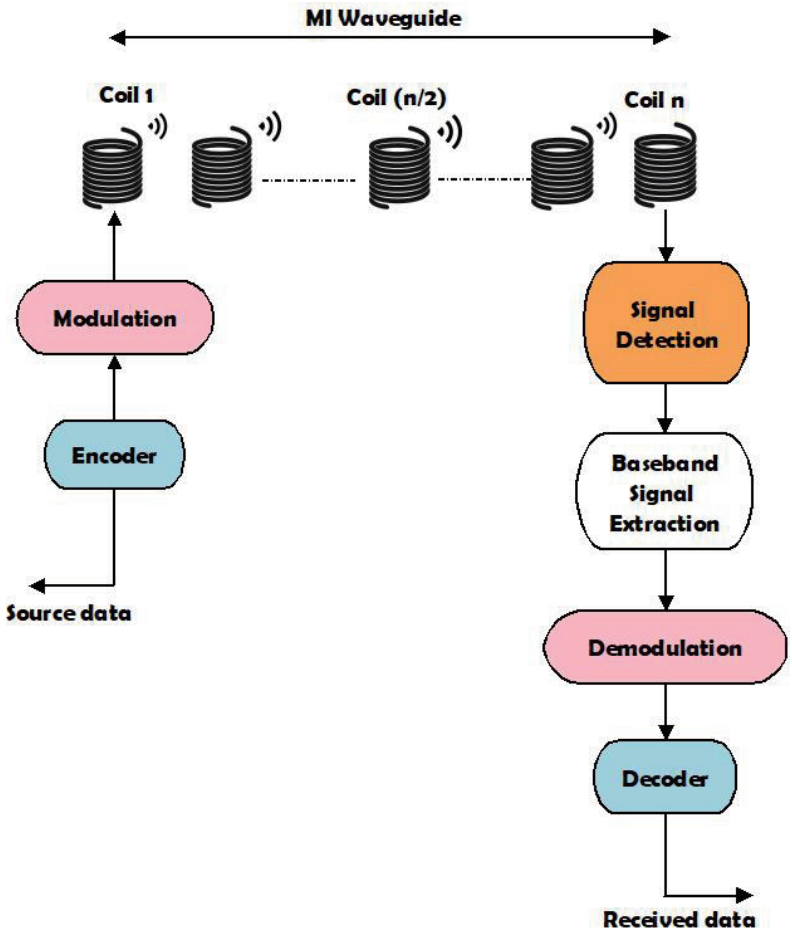

Figure 1. Functional block units of MI waveguide system.

are active, which are powered by external supply, and the relay coils are passive, having no external powering. However, in the above work, single layer coils (SLCs) are used. When being observed for a multilayer coil (MLC) the inductance, magnetic flux characteristics are higher than that for SLCs. However, in MLCs the resistance is also high. It means that MLCs have a set of features that enhance the transmission characteristics and another set of features that deteriorate the same. So, there is a trade-off in the performance that can be achieved by using MLCs. Addressing this trade-off, the transmission range of MI waveguide system is enhanced using MLCs [10]; however, the bandwidth is observed to be low which is up to 1 kHz. In [11–13], the authors developed techniques with which the channel capacity and throughput can be enhanced. Herein, the coils are strongly coupled which requires more number of coils during deployment. However, there are some time critical applications where a large volume of data needs to be sent in less amount of time, e.g., constrained border patrol, mine disaster detection.

To cater the needs of such applications, especially in a loosely coupled scenario spread resonance (SR) strategy is incorporated in MI waveguide system to increase the channel bandwidth [14]. Herein, the authors considered SLCs and dc resistance. Extending this work, in this article we have incorporated MLCs in SR strategy based MI waveguide system. To obtain a more approximated estimate of system performance, we incorporated the impact of ac resistance, skin and proximity effects, and parasitic capacitance as these factors affect the mutual coupling between coils that in turn affect the path loss experienced.

In this paper, in the first part, we tried to enhance the bandwidth of MLC based MI waveguide system by incorporating the existing SR strategy. Besides, in the case of MLCs, different possible structures are possible, and each one has different electro-magnetic characteristics. So, choosing an

optimal MLC can offer better MI system performance. With this observation, in the second part, we focused on developing a more promising MLC structure. To this end, we designed an MLC structure termed as thin-width rectangular coil (TWR coil) and quantitatively compared its characteristics with the existing coils namely solid circular coil and hollow circular coil. These MLC structures are designed in ANSYS MAXWELL R1.21 simulation software. The proposed MLC structure has promising characteristics of low impedance, comparable inductance, and higher magnetic flux. For the proposed coil, we also studied the influence of variation of pitch so as to reduce impedance further.

The rest of the paper is organized as follows. In Section 2, the preliminaries of MI waveguide model, SR strategy, and eddy current effects are explained. In Section 3, the results comprising the channel capacity enhancement and simulation based comparative analysis of three different multi-layer coil structures are explained. Section 4 ends with conclusion and future scope.

2. PRELIMINARIES

In this section, the basics of MI waveguide communication, SR strategy, and eddy current effects in multilayer coils are explained. The former concept is necessary to understand how the channel capacity can be enhanced with this strategy, and the latter is the basis using which the MLC structures are designed and analyzed in this work.

2.1. Spread Resonance Strategy

In conventional MI waveguide system, all the relay coils are tuned to a common resonating frequency. Contrary to this, in SR strategy each relay coil is tuned to distinct resonating frequency which deviates by a very small value called spread intensity (Δf) in adjacent coils [14]. This small deviation is chosen carefully so that the power is spread over a band of frequencies, and there will be minimal path loss. The advantage of this method is that the channel bandwidth can be significantly enhanced by a proper choice of spread intensity. However, the limitation is that the path loss will be greatly increased if the resonating frequencies are widely spread. In this method, to have maximum possible mutual induction the central operating frequency has to be as high as possible. However, due to the high frequency the stray capacitance and eddy current effects become prominent.

In the considered MI waveguide scenario, the coils are sufficiently apart, and thus assuming non-interference from any other pairs of transceivers, the channel capacity (CC) of a communication channel is given as follows

$$CC = B \cdot \log_2 \left(\frac{P_{Tx}}{P_N \cdot L_P} \right) \tag{1}$$

where P_{Tx} is the transmitted power in Watts, P_N the ambient noise power, L_P the system path loss, B the channel bandwidth (Hz), and CC the system channel capacity measured in bits/s. For underground medium given in [15], the value of noise power is -105 dBm. As observed in the work done in [8], the MI waveguide system path loss depends on operating frequency (f_0). Accordingly, the above equation can be rewritten as below.

$$CC = \int_{f_0 - B/2}^{f_0 + B/2} B \cdot \log_2 \left(\frac{P_{Tx}}{P_N \cdot L_P(f)} \right) df \tag{2}$$

In SR strategy, the resonating frequencies of each coil are assigned as $f_0 - \frac{n}{2}\Delta f$, $f_0 - (\frac{n}{2} - 1)\Delta f$, $f_0 - (\frac{n}{2} - 2)\Delta f$, ..., f_0, ... $f_0 + (\frac{n}{2} - 2)\Delta f$, $f_0 + (\frac{n}{2} - 1)\Delta f$, $f_0 + \frac{n}{2}\Delta f$.

From the above resonating frequency assignment, the total system bandwidth is given by

$$BW = n\Delta f \tag{3}$$

where n is the total number of coils including transmitter and receiver, which is taken as even for the sake of convenience. By utilizing the high-frequency multi-transformer model, the path loss of MLC waveguide can be calculated.

From the above Fig. 2, U_{M_i} represents the root mean square value of the voltage induced through magnetic induction in ith coil. Z_{ab} represents the coupled impedance, the influence of coil a on coil b

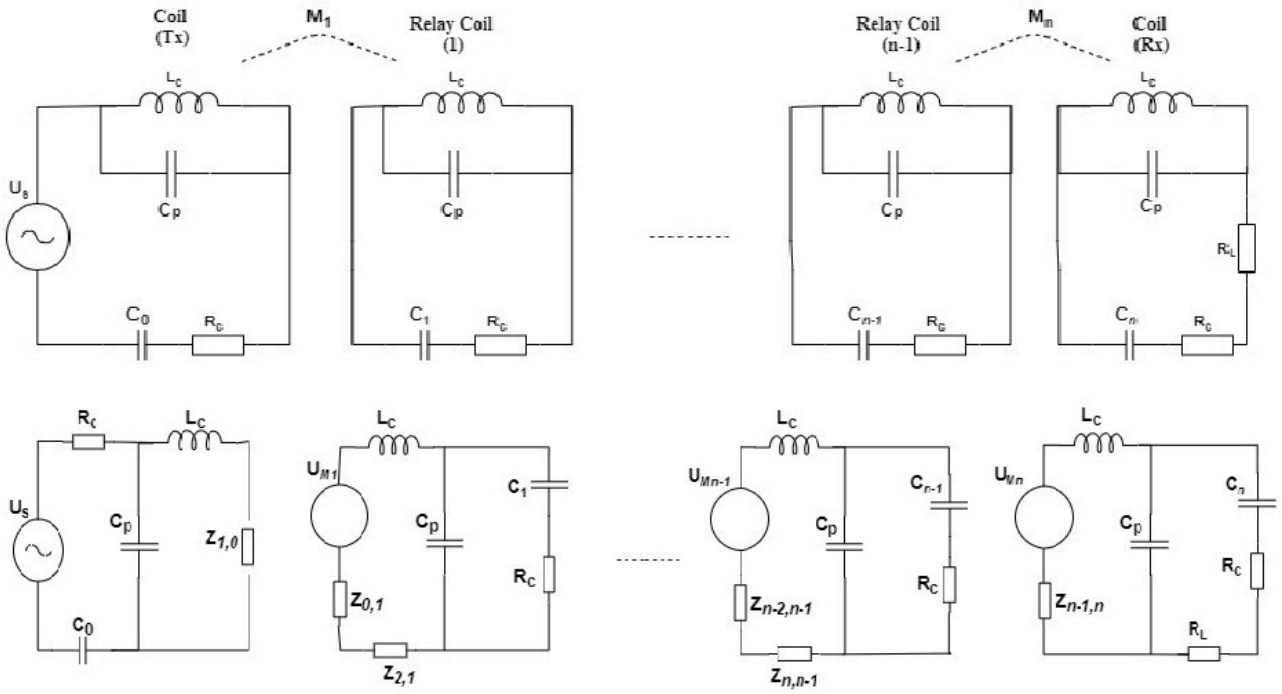

Figure 2. High frequency model of MI waveguide and its equivalent circuit.

and vice-versa. C_i is the external capacitor meant for achieving the resonant status of the coil. Here L_c is the MLC inductance which is given as follows [16, 17].

$$L_c = 2L_{ss}[\frac{(N_t b+1)^{c+2}-1}{b^2(c+1)(c+2)} - \frac{N_t}{b(c+1)}] \tag{4}$$

where N_t, N_l refer to the number of turns and layers of MLC respectively; L_{ss} is the inductance of single spiral; b and c are constants given by [10]

$$\begin{aligned} b &= -0.1049 + 1.2334N_l^{-1} + 0.8443N_l^{-2}, \\ c &= -0.5723 - 0.4298N_l + 0.1126N_l^2 + 0.0134N_l^3, \\ L_{ss} &= -0.5723 - 0.4298N_l^{-0.1} + 0.1126N_l^{-0.2} + 0.0134N_l^{-0.3} \end{aligned}$$

C_p is the parasitic capacitance of the considered MLC whose value is perfectly modeled by [18] and is given as

$$C_p = \frac{1}{N^2}\left[C_{tt}(N_t-1)N_l + C_{ll}\cdot\frac{N_t(4N_t^2-1)}{3}\cdot(N_l-1)\right] \tag{5}$$

where $N = N_l \times N_t$, ϵ_r is the relative permittivity of the insulated coating material around the copper conductor; d_0 is the diameter of the wire with insulation; d_{oc} is the diameter of the wire without insulation coating ($d_0 \geq d_{oc}$); and C_{tt}, C_{ll} represent turn-to-turn capacitance and layer-to-layer capacitance respectively given by the equation below.

$$C_{tt} = C_{ll} = \frac{2\epsilon_0\epsilon_r l_t \arctan\left[\dfrac{\left(-1+\sqrt{2}\right)\left(2\epsilon_r + \ln\dfrac{d_0}{d_{oc}}\right)}{\sqrt{\ln\dfrac{d_0}{d_{oc}}\left(2\epsilon_r+\ln\dfrac{d_0}{d_{oc}}\right)}}\right]}{\sqrt{2\epsilon_r\ln\dfrac{d_0}{d_{oc}} + \left(\ln\dfrac{d_0}{d_{oc}}\right)^2}} \tag{6}$$

The work done in [14] considers the dc resistance, but in reality the coils are excited by an alternating current source. Thus, it is necessary to consider the ac resistance which takes into account the skin effect. As per [19], the ac resistance of a MLC is given as follows

$$R_c = \left(\frac{\pi}{4}\right)^{0.75} \frac{4l_w\sqrt{\eta}}{3\pi\delta_w d_{oc}\sigma_w}(2N_l^2+1) \tag{7}$$

where σ_w is the conductivity of the conducting wire; δ_w is the skin depth of the copper winding at a given frequency given by $\delta_w = \sqrt{\frac{2}{\mu\sigma\omega}}$; η refers to the porosity factor that is the ratio of the distance between the centers of adjacent conductors of the same layer (p) to the diameter of the conductor winding without insulation (d_{oc}), $\eta = \frac{p}{d_{oc}}$. The value of η has the maximum of 1, where the insulation coating is very thin. The total length of the winding is given by l_w. As compared to the dc resistance, though the conducting material is the same, due to skin effect the effective resistance (ac resistance) increases [20]. The coils are assumed to be deployed with all the axes aligned, and accordingly the mutual induction (M_i) between two coils is adopted from [10]. For such a system, by considering the resonant condition scenario, the MI waveguide system channel capacity is given as follows [14]

$$CC = n\Delta f\left[\log_2\left(\frac{P_{Tx}\cdot R_c^2}{4\omega P_N L_c}\right) + 2\sum_{i=1}^{n}\log_2|\omega M_i| - 2\sum_{i=1}^{n}\log_2\left|\frac{R_c}{2} + j2\pi(1-2i)\Delta f\cdot L_c\right|\right] \tag{8}$$

Here, it can be observed that as the MI coils change their orientations as the time elapses, the mutual induction value will be a random variable. It implies that the channel capacity will also be a random variable. In this work, the channel capacity is maximized and measured in terms of outage probability ($Outage_p[CC]$). This measure refers to the channel capacity that the considered MI system can achieve with a probability of $1-p$. Also, here it is assumed that the deviation of inter-coil distances is within tolerance limit, because the coil radius is smaller than the inter-coil distance. Assuming that each of the coils has a direction which is independent and identically distributed, the MI channel capacity can be approximately seen as a Gaussian random variable. In the channel capacity expression, only the second term is a random variable, and it approximately follows normal distribution. Following that, the mean value of the MI channel capacity can be expressed as

$$E[CC] = n\Delta f\left[\log_2\left(\frac{P_{Tx}\cdot R_c^2}{4\omega P_N L_c}\right) + 2n\cdot\log_2(2\pi f_0\cdot|M_0(f_0)|) - 2\sum_{i=1}^{n}\log_2\left|\frac{R_c}{2} + j2\pi(1-2i)\Delta f\cdot L_c\right|\right] \tag{9}$$

where $M_0(f_0)$ is the designed direction of each coil. In our work, we assume that the coil is horizontally deployed (coil axis is horizontal). In this kind of deployment, the mutual induction between consecutive coils will be maximum. Now the outage channel capacity is defined as shown below, where the variance of the MI channel capacity $Var[CC]$ is not possible to analytically calculate because it depends on specific environment and application which vary from case to case. Therefore, the variance is set to $x\%$ of the mean channel capacity, where the value of x defines how severely the coils may deviate from the predefined direction.

$$Outage_p[CC] = E[CC] + erf^{-1}(2p-1)\cdot\sqrt{2\cdot Var[CC]} \tag{10}$$

On the other hand, making an optimal suitable combined choice of operating frequency and intensity spread that can offer maximum system performance is a challenge. This is found out by solving the optimization problem mentioned below.

$$\begin{aligned} &Find:\ f_0,\ \Delta f \\ &Maximize:\ Outage_p\,[CC] \\ &Constraint:\ f_0 + \frac{n}{2}.\Delta f \le \frac{1}{2\pi\sqrt{L_c C_p}} \end{aligned} \tag{11}$$

The above constraint is because the external capacitor should be greater than the parasitic capacitance. The above nonlinear problem can be solved by using convex optimization methods.

2.2. Eddy Current Effects in the Coil

The skin effect and proximity effect are two consequences of eddy currents in a conductor. Both these eddy current effects cause a nonuniform distribution in the conductor cross-section and thus cause winding loss, which increases as the frequency increases. Between the two effects, for an orthogonal coil winding, the increase in ac resistance due to proximity effect is 2.5 times greater than that caused by skin effect [21]. Hence, it is important to reduce these effects as much as possible to minimize the power losses that occur in MI communication [22]. The skin and proximity effects can be reduced by using some of the following ways [23, 24], viz., 1. By increasing the distance between the adjacent conductors, 2. By using a thin cross-section of conductor, 3. By reducing the frequency and increasing the voltage, and 4. By using the ACSR (Aluminium Core Steel Reinforced) conductor. In this work, we investigated using the first two methods mentioned above; accordingly we varied the pitch of the coil and objectively studied and comparatively analysed three different multi-layer coils.

3. RESULTS AND ANALYSIS

In this section, firstly the performance of MI waveguide system using SR strategy is evaluated using programming done in MATLAB R2021b. Herein, the system bandwidth and channel capacity are enhanced. Secondly, a new MLC structure is designed, and its characteristics are comparatively analyzed with the existing solid circular coil and tubular coil by means of ANSYS Maxwell 2021 R1 simulations.

3.1. Channel Capacity Enhancement

In this first part, to study the performance of considered system, the following set of values is considered. The MLC has an inner radius of $a = 0.15\,\mathrm{m}$, and the outer radius varies according to the number of layers. The MLCs are deployed at an equal interval of $r = 4\,\mathrm{m}$. The total number of coils (n) is calculated based on the total transmission distance (d) given by $n = \lceil \frac{d}{r} \rceil + 1$. The conducting wire is made up of copper with a conductivity of $58.7 \times 10^6\,\mathrm{S/m}$. The copper winding has a cross-sectional diameter of 4 mm and an insulating coating of thickness 2 mm. The unit length resistance of copper wire is taken as per AWG 6 standard as $0.0013\,\Omega/\mathrm{m}$. The conductivity of communication medium (soil) is $0.0005\,\mathrm{S/m}$. The relative permittivity of the insulation material of the winding is 2. The transmission power is set to 10 dBm, and the background noise is considered to be $-105\,\mathrm{dBm}$. To characterize the random direction of coils, the variance of channel capacity is taken as 20% of mean value of channel capacity [8, 14].

In Fig. 3, the 20% — outage channel capacity is given as a function of transmission distance. Herein, the influence of coil layers is analyzed. It is interesting to observe that the channel capacity with SR strategy increases at first and then decreases eventually. This initial rise is due to using more relay coils. In other words, with more relay coils there will be more spread in the resonant frequencies, and it will obviously increase the channel capacity. However, this does not increase indefinitely, rather after a particular distance the channel capacity starts decreasing. This is because the system path loss dramatically increases after reaching a threshold of distance. The decline in the performance is also because of considering 20% deviation of coil orientations from their mean positions. Besides, it can be observed from the graph that as the number of layers increases there is a decline in the performance curves. This is because, as shown in above Table 1, with an increase of coil layers there is a considerable increase in the ac resistance which is approximately 100 times more than the dc or ohmic resistance, which actually contributes to the path loss.

Similarly, in Fig. 4, the channel capacity is given as a function of transmission distance, but in this plot we studied the influence of the turns of coil on the MI waveguide system performance. Herein, as the number of turns is increased, the channel capacity is decreased. This is because of the increase in parasitic capacitance as shown in Table 1. In SLCs, as we increase the number of turns the parasitic capacitance decreases, which is contrary in the case of MLCs [18], wherein by increasing the number of turns the parasitic capacitance increases, and by increasing the number of layers, the parasitic capacitance decreases. Owing to the increase in parasitic capacitance, the strength of coupling between two consecutive coils decreases. Thus, from the view point of parasitic capacitance, an MLC with small length (less turns) and more layers is preferred. However, it should be noted that having more number

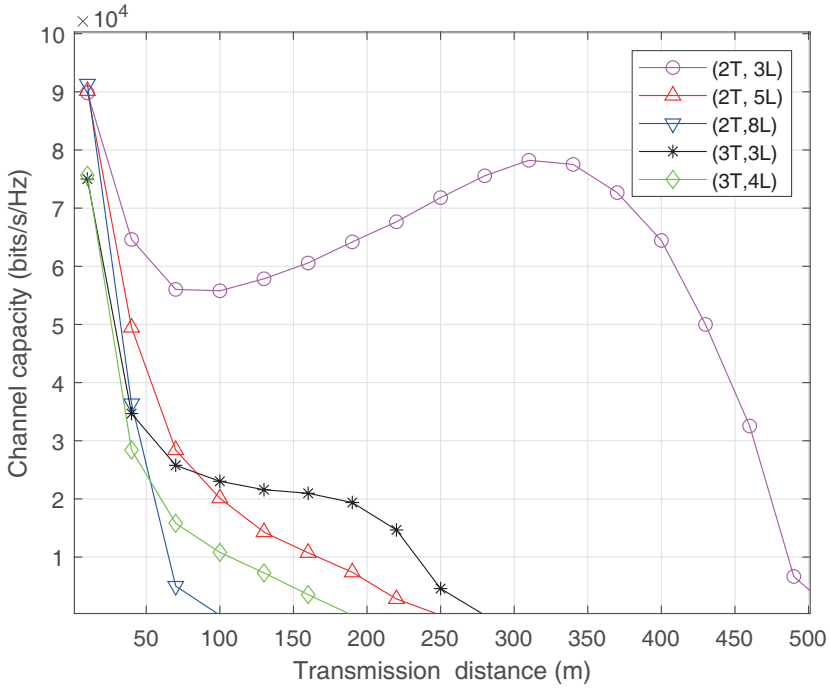

Figure 3. Influence of coil layers on channel capacity performance.

Table 1. Parametric comparison of SLCs and MLCs.

Coil type	N_t	N_l	R_{dc} (Ω)	R_{ac} (Ω)	C_p (pF)	L_c (μH)
Single-layer coil	5	1	0.0061	0.5096	1.940	7.4
	10	1	0.0123	1.0191	0.862	29.6
	15	1	0.0184	1.5287	0.554	66.6
	20	1	0.0245	2.0382	0.408	118.4
Multi-layer coil	2	2	0.0050	0.6278	13.363	25.6
	2	3	0.0077	1.3597	11.671	44.4
	2	5	0.0136	3.8345	8.626	85.4
	2	8	0.0233	10.400	6.253	146.5
	3	2	0.0075	0.9417	19.301	50.8
	3	4	0.0159	3.6321	14.688	134
	4	2	0.0101	1.2555	25.053	81.4
	8	2	0.0201	2.5111	48.294	240.0

of layers increases the ac resistance, and more number of turns increases the stray capacitance. By combining the above two observations from both the graphs, it can be concluded that an MLC with fewer turns and fewer layers offers optimal MI waveguide system performance. Thus, in these graphs we observe that coils with (2T, 2L), (2T, 3L) offer remarkable transmission range.

In the previous two curves, the spread intensity (SI) is kept constant (20 Hz). Now in Fig. 5, the variation of spread intensity on system channel capacity is presented. It can be seen from the graph that when the spread intensity value is relatively low, there is better system performance in terms of channel capacity. This is because, when the spread intensity is low, the adjacent coils will tune frequencies very close to each other that results in a higher power transfer from the preceding coil,

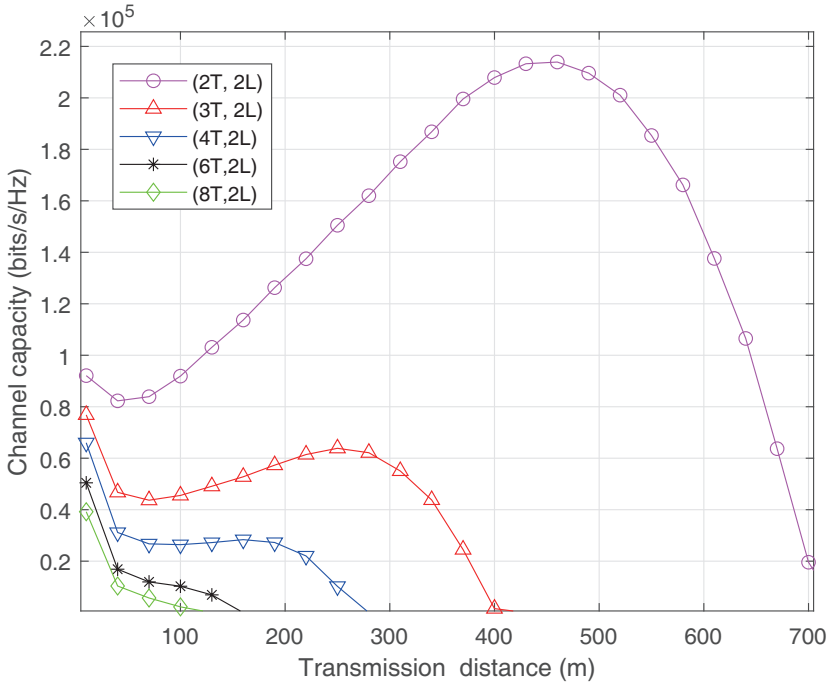

Figure 4. Influence of coil turns on channel capacity performance.

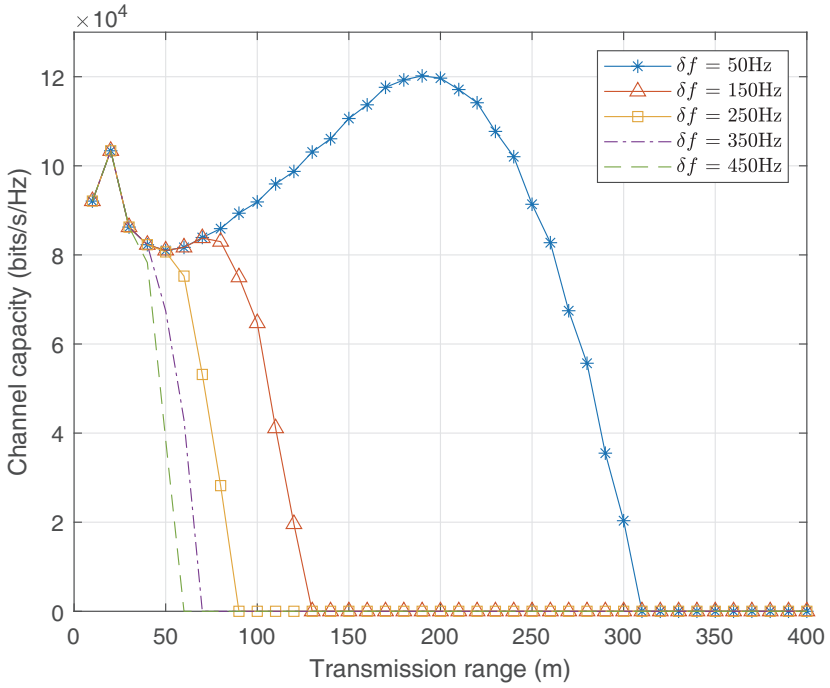

Figure 5. Influence of spread intensity on channel capacity performance.

due to which more number of relay coils can be accommodated in the MI waveguide. However, by keeping the spread intensity a low value, the channel capacity cannot be increased indefinitely. After some threshold number of relay coils, the path loss becomes more prominent, and thus there is decay in the curve after 200 m distance as shown in Fig. 5. On the other hand, when the spread intensity is high, the power difference between two successive coils will be high, and consequently, after a few

relay coils, the transferred power reaches below the half power threshold (3 dB) points. This is why the channel capacity curves exhibit poor performance at higher values of spread intensity. From this curve, the designer gets the idea of a proper choice of external capacitance to achieve a desired operating frequency and spread intensity.

In Fig. 6, the trade-off between the achievable bandwidth and maximum transmission range is shown. In the work mentioned in [10], the system bandwidth is observed to be less than 1 kHz. After incorporating SR strategy, it is increased up to 6 kHz. The reason for this bandwidth raise is due to the spread of operating frequencies, and as a result the power is distributed among a range of frequencies. Thus, the bandwidth increases as explained in (3). Moreover, from this curve it can be observed that for a given spread intensity there is a corresponding bandwidth and transmission range. Specifically, if the spread intensity is higher (say 350 Hz), then very few relay coils can be accommodated. Thus, a smaller transmission range is achieved with a higher bandwidth. On the other hand, if the spread intensity is low (say 50 Hz), then more number of relay coils are accommodated. As a result, a larger transmission range is achieved, but the bandwidth will be less than the former case. Therefore, from this graph the MI waveguide designer can get an idea of proper choice of spread intensity for a desired bandwidth and transmission range specification. By interpolating this graph, it should also be noted that even the lowest bandwidth is around 3.5 kHz, and thus it can be concluded that by incorporating SR strategy, there will be substantial increase of system bandwidth and channel capacity. This strategy works well in media like dry and wet soil where the coil deviations are minimal due to non-moving solid medium. In media like crude oil or water, where the medium is very shaky, not only does the coil orientations deviate greatly but the inter-coil distances also vary remarkably. In such media, SR strategy may not perform well due to more coil deviations.

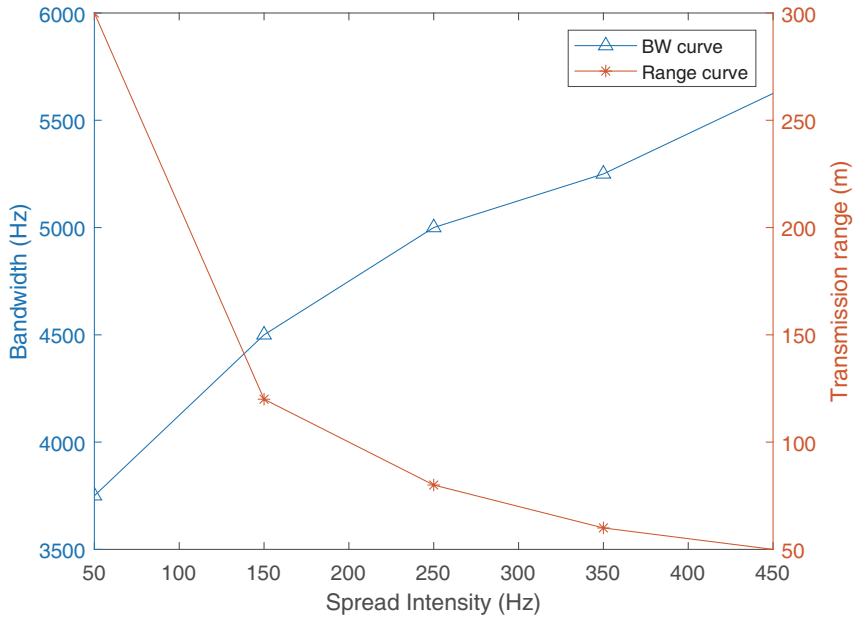

Figure 6. Trade-off between bandwidth and transmission range.

3.2. Comparative Study of MLC Structures

In this second part, we consider three different MLC structures namely solid circular coils, hollow circular coils, and thin-width rectangular coils. The characteristics of each of the coils are objectively studied, and the observations are tabulated subsequently. The coil with optimal characteristics is found out.

3.2.1. Solid Circular Coil (Standard)

The solid circular coil is a standard coil made up of solid copper wire with a circular cross-section of the wire. Besides, the geometry of the coil is also circular. The copper wire is covered by an insulating material which has high dielectric constant and has no magnetic effect. Thus, in all the figures of simulation, the air gap between two windings is considered to be insulation material. In a coil, the distance between the centres of two consecutive windings of same layer is termed as pitch. Similarly, the distance between the centres of windings of two consecutive layers is termed as inter-layer distance as shown in Fig. 7. Both of these physical parameters are crucial in controlling the proximity effect. Increasing either pitch or inter-layer distance reduces the proximity effect.

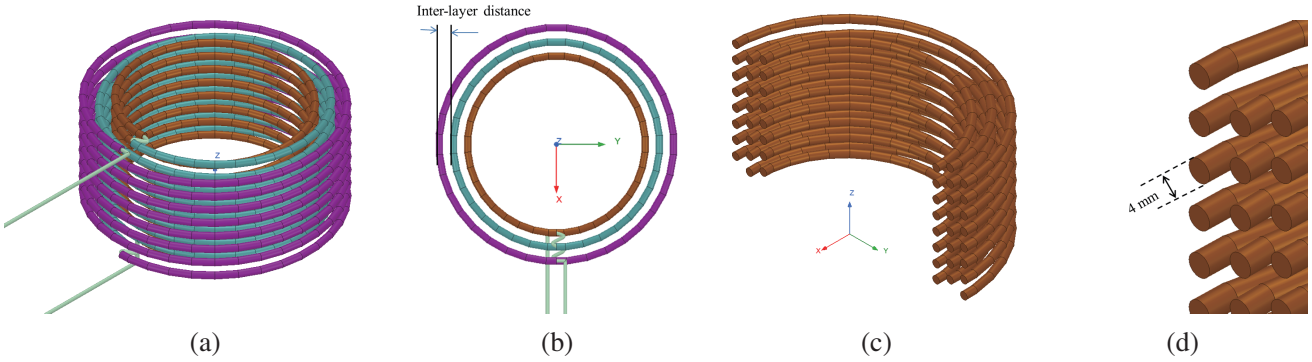

Figure 7. Solid circular coil.

In the simulation, the coil is placed on XY plane with the coil turns advancing in the direction of Z-axis. The inner layer and higher radii layers are connected in series. In other words, layer 1 is connected in series with layer 2, and layer 2 is connected in series with layer 3. Due to this, the current in the coil flows in the same direction throughout. As shown in Table 3, the pitch is varied to three different values, and the corresponding coil characteristics are observed. For all the considered coils, the coil dimensions are taken as follows. Wire diameter is taken as 4 mm; the total turns and layers are 8 and 3, respectively; the pitch is varied in three levels 8 mm, 12 mm, 16 mm ; the inner radius of coil is 50 mm; and inter-layer distance is set as 8 mm.

3.2.2. Hollow Circular Coils (Tubular)

The hollow circular coil (tubular coil) is made up of hollow copper winding with inner radius slightly lesser than the outer radius. In these coils also, the coil diameter is circular. Both the tubular coils and solid circular coils occupy three dimensional space; however, the tubular coils are built with lesser copper material. In this particular tubular coil, the difference between inner and outer radii of the winding is taken to be 0.5 mm as shown in Fig. 8. It can be further reduced. This difference should

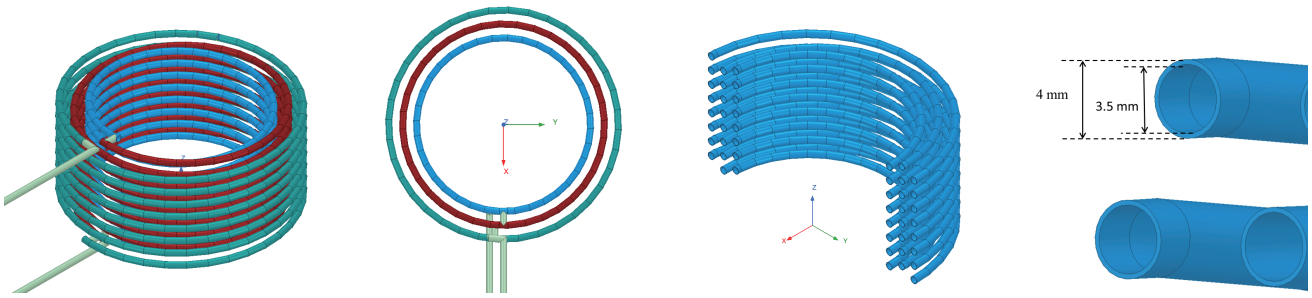

Figure 8. Hollow circular coil.

be greater than the skin depth of copper material at a given frequency. Besides the afore-mentioned specifications, the tubular coil winding has outer radius (r_0) of 2 mm and inner radius (ri) of 1.75 mm.

3.2.3. Thin-Width Rectangular Coil (TWR)

The TWR coil is made up of copper winding with rectangular cross-section. In these coils also, the coil diameter is circular. One turn or strip of this coil resembles a cuboid with thin breadth and small height. Besides the afore-mentioned specifications, the TWR coil winding has a height of 5 mm and a width of 1 mm as shown in Fig. 9. The width of 1 mm is taken here so that it can offer necessary firmness while the coil is prepared. The actual radius of the physical coil is 150 mm, but in simulation we considered only 50 mm radius, for the sake of reducing the simulation time. The motivation behind these simulations is to comparatively study the relative performance of the three considered coils. Though the size is reduced, the relative performance will be the same.

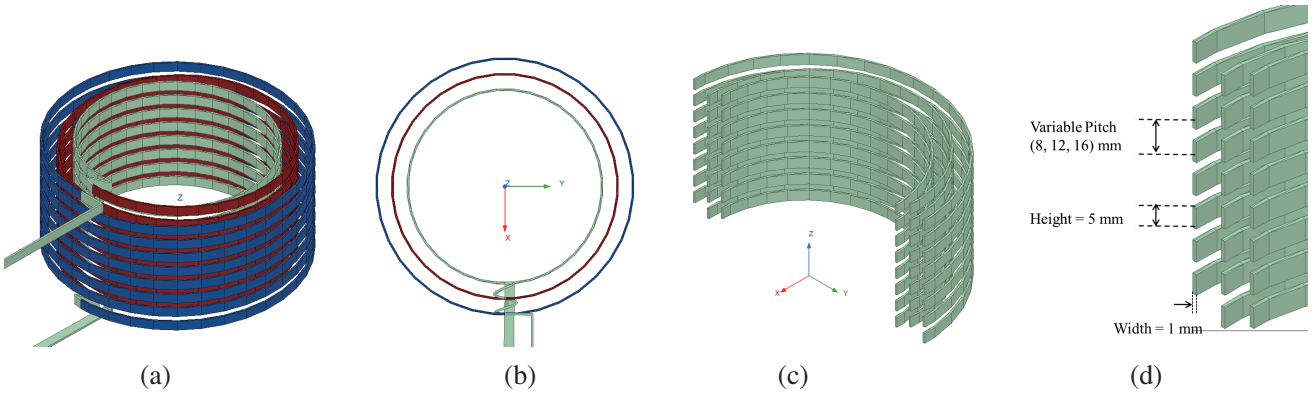

Figure 9. Thin-width rectangular coil. (a) Isometric view. (b) Top view. (c) Cross-sectional view. (d) Coil dimensions.

Here below, the simulated results are tabulated, and based on the observations we tried to conclude the best suitable MLC structure. For comparative analysis, we considered one turn of each kind of MLC and calculated the respective volume and surface area as shown in Table 2. Surface area decides the amount of flux that is finally generated. Volume decides the amount of copper material needed to design the coil.

Table 2. Volume and surface area of 1 turn of each coil.

Coil type	Volume (mm^3)	Surface area (mm^2)
Solid circular coil (standard)	3947.8	3973
Hollow circular coil (tubular)	925.3	3953.7
Thin-width rectangular coil (TWR)	1570.8	3780

For the considered coil dimensions, it can be observed and inferred that $Vol_{standard\text{-}coil} > Vol_{TWR\text{-}coil} > Vol_{Tubular\text{-}coil}$. Slightly different from this, $surface\text{-}area_{standard\text{-}coil} > surface\text{-}area_{Tubular\text{-}coil} > surface\text{-}area_{TWR\text{-}coil}$.

It can be seen from Table 3 that as the pitch of the coil is increased, the impedance is further reduced even though the copper material is unchanging. This is because of reduced proximity effect. As the turns of the coil are stretched outwards, the pitch increases, and the proximity between two turns decreases. Eventually, the impedance due to proximity effect also decreases. However, as the pitch increases, the inductance value gets reduced because the increased pitch makes the winding close to a straight long conductor whose inductive effect is low. Besides, the increase of pitch creates spaces between the copper windings. This leads to a leakage of flux that is not intersected by the windings. This

Table 3. Characteristics of different types of coils with variation of pitch.

Coil type	Pitch (mm)	L (μH)	Z (kΩ)	Flux (μWb)
Solid circular coil	8	49.47	$0.000289 + 1.554i$	247
	12	39.52	$0.000207 + 1.242i$	198
	16	33.50	$0.000172 + 1.051i$	168
Hollow circular coil	8	44.41	$0.000236 + 1.395i$	222
	12	38.94	$0.000169 + 1.223i$	195
	16	31.84	$0.000132 + 1.002i$	159
Thin-width rectangular coil	8	50.31	$0.000137 + 1.581i$	252
	12	40.43	$0.000082 + 1.271i$	202
	16	34.37	$0.000062 + 1.079i$	172

leads to reduction in the magnetic flux generated. Owing to the above reasons, as the pitch is increased in all the three MLC configurations, the inductance, impedance, and generated magnetic flux decrease. Though the impedance is reduced which is favourable for reducing the power loss, the reduction in inductance and magnetic flux negatively affects the strength of coupling between consecutive coils in MI communication. So, optimal pitch needs to be chosen as per the application requirements. We consider a sinusoidal current of 5 A at a frequency of 5 MHz. For a copper coil, at this frequency the skin depth is 29.3 micro-meters. It means that in the considered tubular coil a thickness of 0.47 mm (0.5 mm–29.3 μm) does not carry any current density. Thus, the thickness of the tubular coil can be further reduced without compromising the strength of the coil structure (thin tubular structures can break or result in sharp bends while preparing a coil).

3.2.4. Tubular Coil Versus Standard Coil

One of the major advantages of tubular coils over standard coil is the lesser material cost. From Table 3, as compared to standard coils, it is observed that tubular coils offer low impedance, less material cost, relatively less magnetic flux, and less inductance. Even though both the coils have same skin depth that is related to the conduction path, the slightly different impedance value is because of the following reasons. As shown in Fig. 7 and Fig. 8, while performing simulation, for standard coil, thin conductors having a cross-sectional diameter of 2–3 mm are drawn out of their faces and are excited with ac input, where as in tubular coils, to facilitate proper impedance matching tubular conductors having same cross-sectional diameter of 4 mm (identical to the cross-section of coil winding) are drawn out. Owing to this, in tubular coils, the current has relatively a larger conduction path, and thus the resistance value is seen to be lesser than that of standard coil.

3.2.5. TWR Coil Versus Standard Coil

From Table 3, as we compare the TWR coils with the standard coils, TWR coils offer very low impedance, lesser material cost, slightly higher magnetic flux, and approximately identical inductance. From the comparison calculations shown in Table 2, it is very clearly seen that the volume or the material required to make a TWR is less than that of standard coil. Nevertheless, the characteristics of TWR are more promising than standard coil. This is due to the following reasons. As per $\Phi = BA\cos(\theta)$, the flux (Φ) generated through a conducting surface depends on the surface area of conductor (A) and magnetic field lines that cut the conductor and the orientation (θ) between the surface normal and the magnetic field vector (B). With this background, it may be surprising that though the surface area of TWR coil is lesser than the other two coil configurations, the flux generated from TWR coils is higher than the two. This is because, in cylindrical cross-sectional conductors, a part of the field lines intersect the conductor radially, and a few other field lines intersect tangentially. Thus, the overall flux generated

is low. However, in TWR coil, all the field lines intersect the winding perpendicularly ($\theta = 0°$) which result in maximum flux. This is the advantage of choosing a rectangular coil. Furthermore, as the flux generated is high, coil's self-inductance will also be high as per the relation $L = \frac{N\Phi}{I}$, where N is the number of coil turns, and I is the excited current. It consequently results in an increased inductive reactance as shown in Table 3.

3.3. Discussion

From the calculations provided in Table 2, it is evident that though the volume (copper content) of TWR coil is higher than the tubular coil, the characteristics of TWR coil are very promising. From the above observations, it can be concluded that from less resistance point of view, TWR coil > Tubular coil > Standard coil. In other words, by incorporating TWR coils in MI communication, lesser path loss can be achieved. Also, from maximum flux point of view, TWR coil > Standard coil > Tubular coil. Owing to this, TWR coils can offer a higher transmission range due to having a strong mutual coupling. From the economy point of view, Tubular coil > TWR coil > Standard coil. It means that tubular coils can offer reasonably good MI communication performance, but with a little compromise in path loss and transmission range. Therefore, it can be concluded that TWR coils can offer optimal MI communication performance among the three coil configurations. However, TWR coils can be slightly costlier than the tubular coils. In this work, so far we tried to reduce the proximity effect by increasing the pitch of the coil; however, the losses due to this effect can also be reduced by increasing the inter-layer distance. In that case, though the proximity effect gets reduced, there will be a reduction in flux due to flux leakages. There is an upper threshold up to which the inter-layer distance can be increased. This can further improve the system performance.

4. CONCLUSION

In this paper, we achieved higher bandwidth and channel capacity of MI waveguide communication system by incorporating SR strategy. Contrary to the baseline work where SR strategy is first introduced, in this work MLCs are incorporated in place of SLCs. Herein, in order to get a better approximation of performance parameters, the ac resistance associated with MLCs, impact of parasitic capacitance and also the skin and proximity effects are incorporated. The skin and proximity effects arise due to eddy currents in the ac current carrying coil. It is observed that ac resistance is higher than the coil's dc resistance value. Aside from this, there is another skin depth considered in this work, which corresponds to the MI signal behavior in the communication medium. In this mathematical analysis, it is observed that the MLCs with lesser turns and lesser coils can offer higher transmission range and bandwidth as these coils have less ac resistance, less stray capacitance, and sufficient self-inductance value. In this work, the bandwidth is increased up to 6 kHz but with a trade-off with achievable transmission range, and consequently the channel capacity is also increased. This work can be utilized in applications like border patrol and mine-disaster rescue operations, where there is a need for high channel capacity. This work needs further validation with experimental evaluation.

Furthermore, we examined three different MLC configurations namely solid circular coil, tubular coil, and TWR coil, and compared the characteristics like self-inductance, impedance, and magnetic flux generated. After comparing the simulated results, we inferred that tubular coil is an economical option with less copper content which can offer reasonably good performance of MI communication. On the other hand, TWR coil is found to have more favourable features in terms of more energy storing capacity, less resistance, and more flux and inductance. Due to these characteristics, these coils can offer higher transmission ranges and low path loss. Based on these simulation results, we conclude that the TWR coil is the optimal MLC among the three. In this work, the results provided for SR strategy are based on standard solid circular coils. By incorporating TWR coil in MI waveguide system, the performance can be further enhanced. This work is based on simulations performed using ANSYS Maxwell. To further validate the optimal performance of the TWR coil in MI communication, it is needed to mathematically model the self-inductance, parasitic capacitance, and ac resistance of the tubular and TWR coils, which is the future scope of this work.

ACKNOWLEDGMENT

This work is supported by Visvesvaraya PhD scheme under Ministry of Electronics and Information Technology (MEITY), India. The authors would like to thank fellow research scholars Dr. Durgesh, shankar and srinivas for their valuable technical support for this work.

REFERENCES

1. Sharma, A. K., S. Yadav, S. N. Dandu, V. Kumar, J. Sengupta, Sanjay B. Dhok, and S. Kumar, "Magnetic induction-based non-conventional media communications: A review," *IEEE Sensors Journal*, Vol. 17, No. 4, 926–940, 2016.
2. Sandeep, D. N. and V. Kumar, "Review on clustering, coverage and connectivity in underwater wireless sensor networks: A communication techniques perspective," *IEEE Access*, Vol. 5, 11176–11199, 2017.
3. Sun, Z., P. Wang, M. C. Vuran, M. A. Al-Rodhaan, A. M. Al-Dhelaan, and I. F. Akyildiz, "Misepipe: Magnetic induction-based wireless sensor networks for underground pipeline monitoring," *Ad Hoc Networks*, Vol. 9, No. 3, 218–227, 2011.
4. Sun, Z., P. Wang, M. C. Vuran, M. A. Al-Rodhaan, A. M. Al-Dhelaan, and I. F. Akyildiz, "Bordersense: Border patrol through advanced wireless sensor networks," *Ad Hoc Networks*, Vol. 9, No. 3, 468–477, 2011.
5. Sun, Z. and I. F. Akyildiz, "Channel modeling and analysis for wireless networks in underground mines and road tunnels," *IEEE Transactions on Communications*, Vol. 58, No. 6, 1758–1768, 2010.
6. Kumar, V., R. Bhusari, S. B. Dhok, A. Prakash, R. Tripathi, and S. Tiwari, "Design of magnetic induction based energy-efficient wsns for nonconventional media using multilayer transmitter-enabled novel energy model," *IEEE Systems Journal*, Vol. 13, No. 2, 1285–1296, 2018.
7. Tambe, S., V. Kumar, and R. Bhusari, "Magnetic induction based cluster optimization in non-conventional WSNs: A cross layer approach," *AEU-International Journal of Electronics and Communications*, Vol. 93, 53–62, 2018.
8. Sun, Z. and I. F. Akyildiz, "Magnetic induction communications for wireless underground sensor networks," *IEEE Transactions on Antennas and Propagation*, Vol. 58, No. 7, 2426–2435, 2010.
9. Shamonina, E., V. A. Kalinin, K. H. Ringhofer, and L. Solymar, "Magnetoinductive waveguide," *Electronics Letters*, Vol. 38, No. 8, 371–373, 2002.
10. Dandu, S. N., V. Kumar, J. Sengupta, and N. D. Bokde, "Performance analysis of multilayer coil based mi waveguide communication system," *Computers, Materials Continua*, Vol. 72, 5287–5300, 2022.
11. Kisseleff, S., I. F. Akyildiz, and W. H. Gerstacker, "Throughput of the magnetic induction based wireless underground sensor networks: Key optimization techniques," *IEEE Transactions on Communications*, Vol. 62, No. 12, 4426–4439, 2014.
12. Kisseleff, S., W. Gerstacker, R. Schober, Z. Sun, and I. F. Akyildiz, "Channel capacity of magnetic induction based wireless underground sensor networks under practical constraints," *2013 IEEE Wireless Communications and Networking Conference (WCNC)*, 2603–2608, 2013.
13. Sun, Z. and I. F. Akyildiz, "On capacity of magnetic induction-based wireless underground sensor networks," *2012 Proceedings IEEE INFOCOM*, 370–378, 2012.
14. Sun, Z., I. F. Akyildiz, S. Kisseleff, and W. Gerstacker, "Increasing the capacity of magnetic induction communications in RF-challenged environments," *IEEE Transactions on Communications*, Vol. 61, No. 9, 3943–3952, 2013.
15. Etemadrezaei, M., "High quality factor resonators for inductive power transfer systems," North Carolina State University, 2015.
16. Kim, J., B. Kim, J. Kang, and K. Kim, "A novel method for estimating multilayer coil inductance," *IEEE Magnetics Letters*, Vol. 8, 1–4, 2017.

17. Kim, J., K. Kim, B. Kim, and J. Kang, "Experimental validation of multi-layer coil inductance estimation method," *2017 IEEE International Symposium on Antennas and Propagation & USNC/URSI National Radio Science Meeting*, 1303–1304, 2017.
18. Massarini, A., M. K. Kazimierczuk, and G. Grandi, "Lumped parameter models for single- and multiple-layer inductors," *PESC Record. 27th Annual IEEE Power Electronics Specialists Conference*, Vol. 1, 295–301, 1996.
19. Wojda, R. P., "Winding resistance and winding power loss of high-frequency power inductors," 2012.
20. Kaymak, M., Z. Shen, and R. W. De Doncker, "Comparison of analytical methods for calculating the ac resistance and leakage inductance of medium-frequency transformers," *2016 IEEE 17th Workshop on Control and Modeling for Power Electronics (COMPEL)*, 1–8, 2016.
21. Lotfi, A. W., P. M. Gradzki, and F. C. Lee, "Proximity effects in coils for high frequency power applications," *IEEE Transactions on Magnetics*, Vol. 28, No. 5, 2169–2171, 1992.
22. Pantic, Z. and S. Lukic, "Computationally-efficient, generalized expressions for the proximity-effect in multi-layer, multi-turn tubular coils for wireless power transfer systems," *IEEE Transactions on Magnetics*, Vol. 49, No. 11, 5404–5416, 2013.
23. Alabakhshizadeh, A. and O.-M. Midtgxard, "Optimum core dimension for minimizing proximity effect losses of an AC inductor for a galvanically isolated pv inverter," *2012 38th IEEE Photovoltaic Specialists Conference*, 001373–001377, 2012.
24. Brennan, T., "Proximity-effect loss calculations for a discontinuous-mode PFC inductor utilising a multifilar winding construction," *IEE Proceedings-Electric Power Applications*, Vol. 152, No. 5, 1101–1105, 2005.